Position and attitude estimation using tightly coupled multi baseline multi constellation GNSS and inertial sensor fusion

Marton Farkas [1) 2)], Szabolcs Rozsa [2)], Balint Vanek [1)]

Abstract

- Position and attitude determination algorithm
- Tightly coupled sensor fusion for using low-cost multi antenna, multi GNSS and inertial sensor observations
- Post-processed kinematic positioning (PPK) solution with Extended Kalman Filter (EKF) realization
- Real case study with a UAV platform
  - Two low-cost u-blox NEO-M8T GNSS receivers, primary (P), secondary (S)
  - PIXHAWK flight controller computer with INS sensors
  - Sony ILCE-6000 camera for photogrammetric data collection
  - A low-cost u-blox NEO-M8T ground based GNSS base station (B)
- Fusing accelerometer and gyroscope observations with GNSS code, carrier-phase and Doppler observations

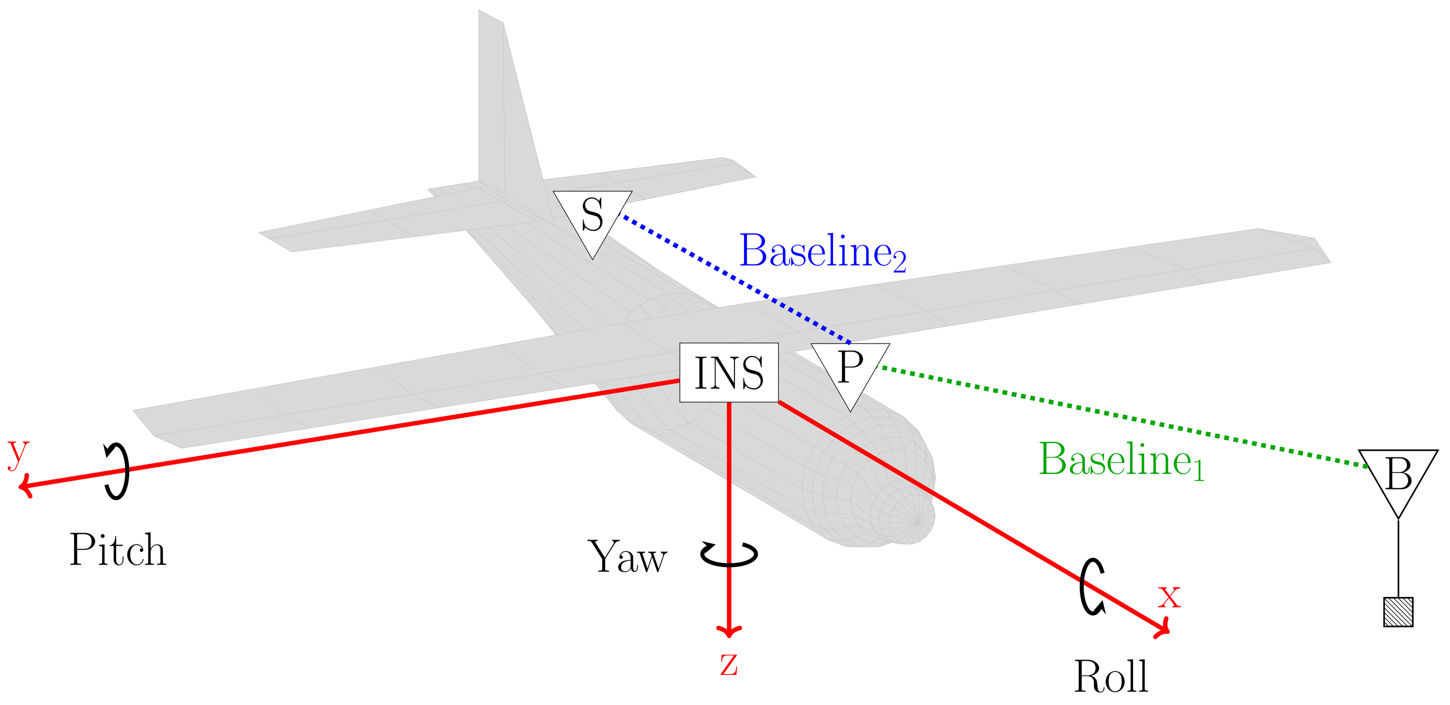

- Positioning of the platform
  - GNSS observations of the first baseline between the base station and the primary receiver
  - Acceleration data
- Quaternion based attitude estimation
  - GNSS observtions taken in the second, moving baseline
  - Gyroscope data
- The integer ambiguities are resolved by the LAMBDA method for the position and a quaternion constrained modified LAMBDA method for the UAVs moving baseline
- The position estimations are compared with the post-processed solution of RTKLIB software
- The attitude estimations are compared with the estimations of the onboard flight controller system and both of them are validated using post-processed attitude information obtained from photogrammetric data processing (PGP) with PIX4D software

Estimation algorithm

The estimation is based on an Extended Kalman Filter algorithm. The estimated states, which are linked to the navigation data and the different sensor errors are

- Position ($\boldsymbol{X_P}$), velocity ($\boldsymbol{V_P}$) and acceleration ($\boldsymbol{A_P}$) of the Primary GNSS antenna in ECEF Coordinate system
- Orientation quaternions ($\boldsymbol{q}$), quaternion derivatives ($\dot{\boldsymbol{q}}$)
- Accelerometer bias error ($\boldsymbol{b_a}$), gyroscope bias error ($\boldsymbol{b_\omega}$)
- GNSS receiver clock biases for every receiver ($\delta_i^{GPS}, \delta_i^{GAL}, \delta_i^{GLO}$)
- GNSS receiver clock drifts for every receiver ($\dot{\delta}_i^{GPS}, \dot{\delta}_i^{GAL}, \dot{\delta}_i^{GLO}$)
- Single differenced inter-channel biases for every baseline ($\boldsymbol{B}$)
- Single differenced integer ambiguities for every baseline and every satellite ($\boldsymbol{N}$)

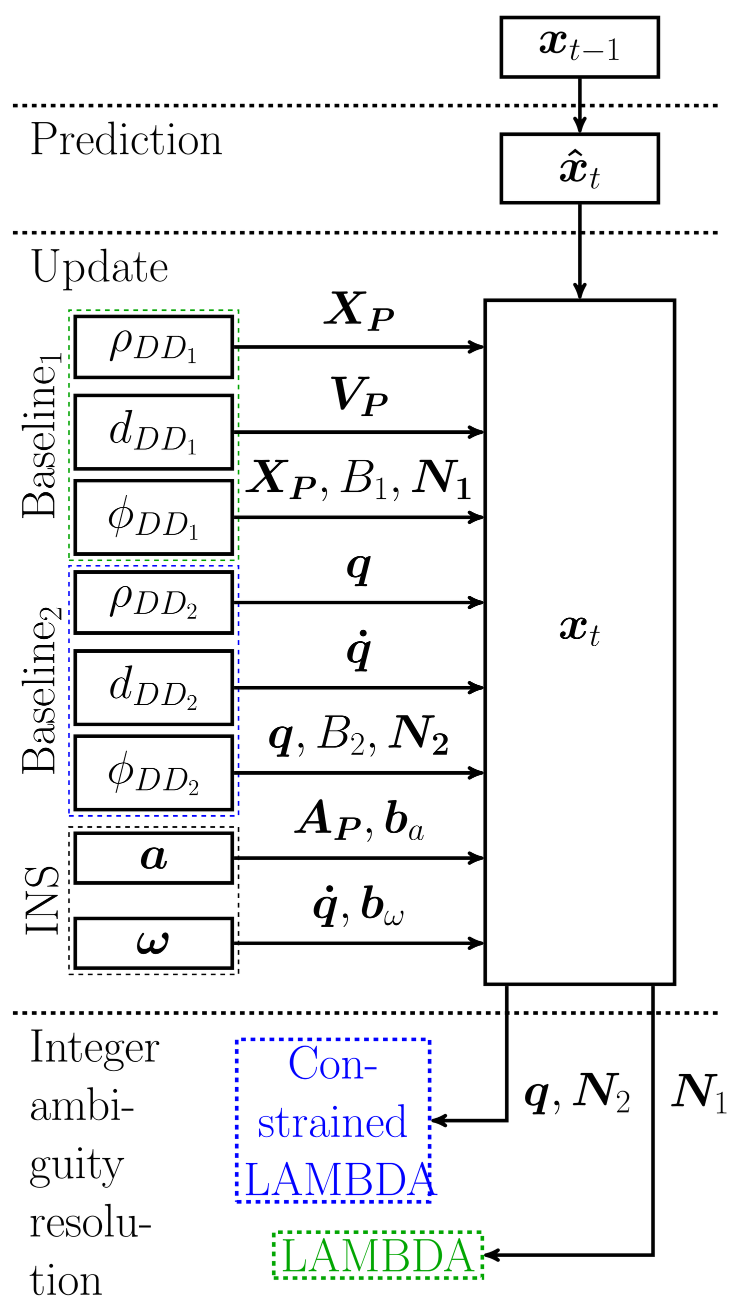

Integer ambiguity resolution

The original LAMBDA minimization problem is used for the first baseline

- The float integer ambiguities in double differenced form ($\hat{\boldsymbol{x}}_{\boldsymbol{N}}$)
- The covariance matrix of the double differenced float integer ambiguities ($\hat{\boldsymbol{x}}_{\boldsymbol{N}}$)
- The optimal integer valued vector of the ambiguities ($\check{\boldsymbol{x}}_{\boldsymbol{N}}$)

$$\check{\boldsymbol{x}}_{\boldsymbol{N}} = \arg \min_{\boldsymbol{x_N} \in \mathbb{Z}^m} \|\boldsymbol{x_N} - \hat{\boldsymbol{x}}_{\boldsymbol{N}}\|^2_{\hat{P}_{NN}}$$

The quaternion constrained LAMDA method for the second, moving baseline

- The first part of the equation is the original cost function part
- The second part represents the quaternion constraint with the conditional quaternion vector ($\hat{\boldsymbol{x}}_{\boldsymbol{q}}(\boldsymbol{x_N})$), its covariance matrix ($\hat{\boldsymbol{P}}_{\boldsymbol{q(N)q(N)}}$) and $\check{\boldsymbol{x}}_{\boldsymbol{q}}(\boldsymbol{x_N})$ in the second part of $C(\boldsymbol{x_N})$ equation is the second optimization

$$\check{\boldsymbol{x}}_{\boldsymbol{N}} = \arg \min_{\boldsymbol{x_N} \in \mathbb{Z}^m} (C(\boldsymbol{x_N}))$$

$$C(\boldsymbol{x_N}) = \|\boldsymbol{x_N} - \hat{\boldsymbol{x}}_{\boldsymbol{N}}\|^2_{\hat{P}_{NN}} + \|\hat{\boldsymbol{x}}_{\boldsymbol{q}}(\boldsymbol{x_N}) - \check{\boldsymbol{x}}_{\boldsymbol{q}}(\boldsymbol{x_N})\|^2_{\hat{P}_{q(N)q(N)}}$$

$$\check{\boldsymbol{x}}_{\boldsymbol{q}}(\boldsymbol{x_N}) = \arg \min_{\|\boldsymbol{x_q}\|^2=1} \|\hat{\boldsymbol{x}}_{\boldsymbol{q}}(\boldsymbol{x_N}) - \boldsymbol{x_q}\|^2_{\hat{P}_{q(N)q(N)}}$$

UAV flight test results

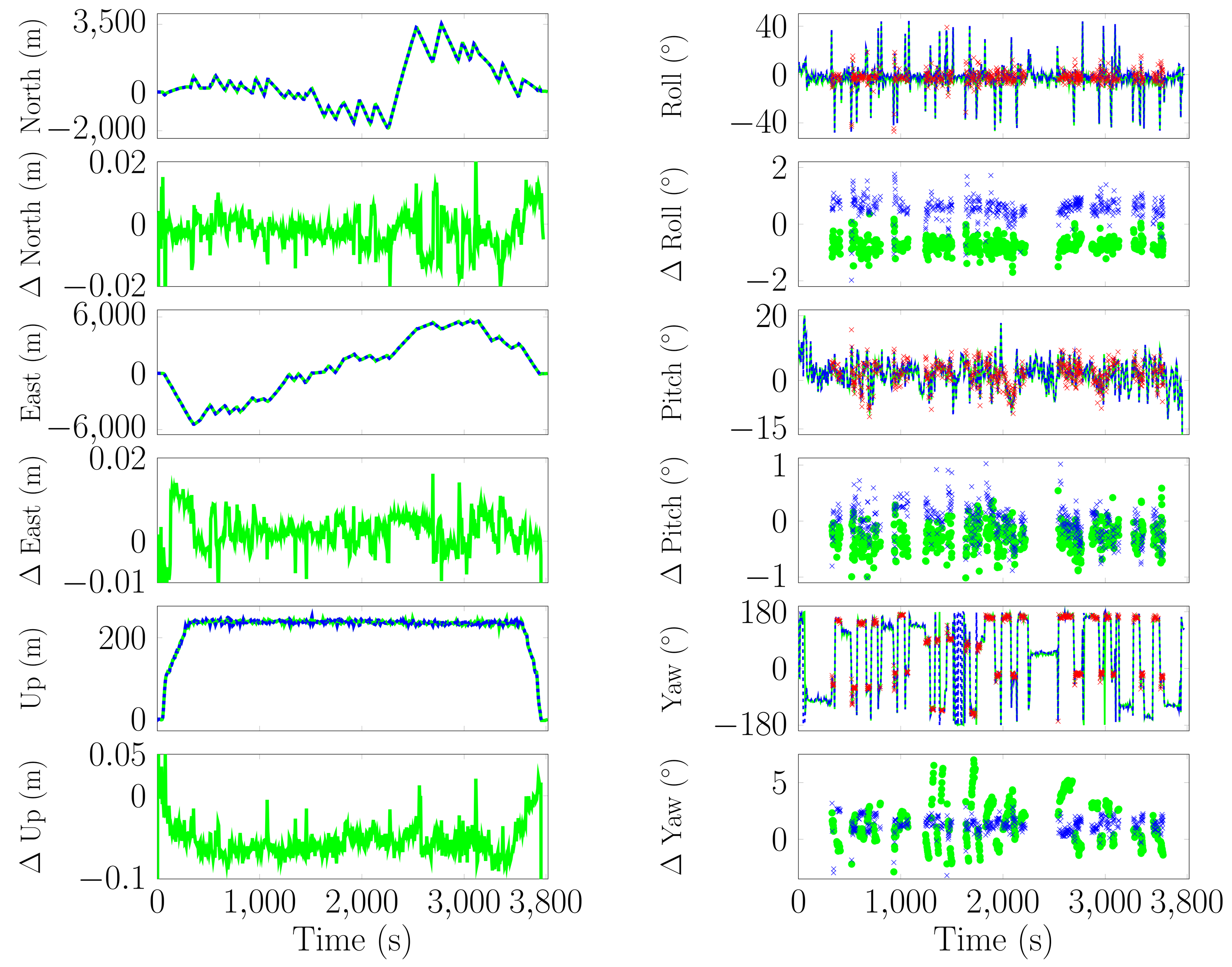

Comparison of the PPK (–) and the EKF (···) coordinate solutions and their differences (Δ)

Comparison of the PGP(·), PIXHAWK (–) and the EKF (···) solution's Roll, Pitch and Yaw angles and the differences from the PGP solution PIXHAWK(·), EKF (·)

		North	East	Up
EKF_{IAR} - PPK coordinates [m]	mean	-0.003	0.002	-0.055
	rms	0.008	0.004	0.059
AR succes rate $Baseline_1$	92.91%			
		Roll	Pitch	Yaw
PIXHAWK - PIX4D Euler angles [°]	mean	-0.72	-0.30	1.27
	rms	0.77	0.42	2.47
EKF - PIX4D Euler angles [°]	mean	0.57	-0.04	1.15
	rms	0.68	0.37	1.71
AR succes rate $Baseline_2$	88.18%			

- The duration of the flight was 3800 seconds
- 7 GPS, 4 Galileo and 7 Glonass satellites were received

- The duration of the flight was 3800 seconds
- 7 GPS, 4 Galileo and 7 Glonass satellites were received
- Integer ambiguities were resolved for GPS and Galileo satellites
- Maximal length of the first baseline was 6 kilometres
- The second baseline was 0.29 meters long
- Sony ILCE-6000 camera took 540 pictures during the flight at several mapping areas for the photogrammetric data acquisition

The project leading to these results has received funding from the European Union's Horizon 2020 research and innovation programme, VISION, contract no. 690811.

VISION

Support of grant BME FIKP-VÍZ by EMMI is kindly acknowledged.

Systems and Control Lab, Institute for Computer Science and Control, Budapest, Hungary [1)]
Department of Geodesy and Surveying, Faculty of Civil Engineering, Budapest University of Technology and Economics, Budapest, Hungary [2)]

Published in: 2019 IEEE International Workshop on Metrology for AeroSpace, MetroAeroSpace 2019. IEEE, Torino, pp. 162-167. ISBN 9781728113432